Plasticity of body axis polarity in *Hydra* regeneration under constraints

Anton Livshits[1 *], Liora Garion[1 *], Yonit Maroudas-Sacks[1], Lital Shani-Zerbib[1], Kinneret Keren[1,2,3 #], Erez Braun[1,2 #]

[*] These authors contributed equally

[#] Corresponding authors

[1] Department of Physics, [2] Network Biology Research Laboratories and [3] The Russell Berrie Nanotechnology Institute, Technion – Israel Institute of Technology, Haifa 32000, Israel

Abstract

One of the major events in animal morphogenesis is the emergence of a polar body axis. Here, we combine classic grafting techniques with live imaging to study the emergence of body axis polarity during whole body regeneration in *Hydra*. Composite tissues are made by fusing two rings, excised from separate animals, in different configurations that vary in the relative polarity and original position of the rings along the body axis of the parent animals. We find that under frustrating initial configurations, body axis polarity that is otherwise stably inherited from the parent animal, can become labile and even be reversed. The site of head regeneration exhibits a bias for the edges of the fused doublets, even when this involves polarity reversal in the tissue, emphasizing the importance of structural factors in head formation. The doublets' edges invariably contain defects in the organization of the supra-cellular actin fibers, which form as the tissue ring seals on each side. We suggest that the presence of a defect can act as an "attractor" for head formation at the edge, even though a defect is neither required nor sufficient for head formation. The observation of head formation at an originally distal edge of the tissue upon polarity reversal, is not compatible with models of *Hydra* regeneration based solely on preexisting morphogen gradients. Rather, our results suggest that body axis determination is a dynamic process that involves mechanical feedback and signaling processes that are sensitive to the original polarity and position of the excised tissues.

Significance statement

The formation of a polar body axis is one of the most basic steps in defining the body plan of a developing animal. Here we study the emergence of polarity in *Hydra* regenerating from composite tissue segments under constraints. We show that these frustrating conditions expose non-trivial dynamics, reflecting the integration of the memory of the tissue's original polarity and position in the parent animal with dynamic biochemical and mechanical processes. In particular, we demonstrate that the organization of the cytoskeleton participates together with biochemical signaling processes in feedback loops that eventually result in the formation and stabilization of the animal's body axis. We conclude that preexisting biochemical gradients in the tissue cannot by themselves explain axis determination.

Introduction

The establishment of a body axis is one of the fundamental initial steps of animal morphogenesis (1). The definition of an axis initiates the patterning process, delineating both the alignment and the polarity of the developing body plan. This is true both in developing embryos and during whole body regeneration in organisms such as planarians or *Hydra*. Whereas in some cases the establishment of a body axis occurs *de novo* and involves a spontaneous symmetry breaking event (2, 3), often there is a strong memory of polarity inherited from the parent animal. The memory of polarity is evident in excised tissues of planaria (4) or *Hydra* (5, 6), which regenerate along the direction of the original body axis, as well as in developing animals such as drosophila where polarity arises from inherited gradients of maternal mRNA in the oocyte (1). Interestingly, the molecular toolbox underlying axis formation in embryonic development and during regeneration is largely shared among different animals, with a central role for the Wnt signaling pathway (1, 3, 4, 7, 8). Despite extensive research over the last few decades, many fundamental questions regarding body axis formation and maintenance in animal morphogenesis remain largely open.

Here we focus on body axis polarity in the small fresh-water animal *Hydra*. *Hydra* have a single polar body axis, with a head at one end and a foot at the other end. This simple uniaxial body plan together with *Hydra*'s remarkable regeneration capabilities make it an excellent model system to explore fundamental concepts related to the establishment and maintenance of body axis polarity. Indeed, classic work in *Hydra* was instrumental in shaping our current understanding of axial patterning, establishing the important role of an "organizer" (6, 9), and putting forward the idea of pattern formation by reaction-diffusion dynamics of morphogens (10-12) and the concept of positional information (13-15).

Extensive previous work has shown that the body axis – both its alignment and its polarity – are strongly preserved in regenerating *Hydra* tissues. The memory of polarity in *Hydra* was first demonstrated by Abraham Trembley, who in 1744 showed that bisected *Hydra* can regenerate a head or foot according to their original polarity (16). Later work showed that the memory of polarity is retained even in small excised tissue segments (5, 17). Despite this memory, the polarity of regenerating *Hydra* tissues can also exhibit substantial plasticity under certain conditions (18-21). For example, gastric tissue pieces can exhibit polarity reversal in response to local pharmacological perturbations (21) or be induced to switch polarity by grafting a head and a foot in the opposite polarity (19, 20).

The central player in the maintenance of the polar body axis in *Hydra* is the head organizer, located at the tip of the hypostome in the head of mature animals (6, 9). The organizer activity is thought to be autocatalytic and produces both activation and inhibition signals that form morphogenetic gradients originating from the head and extending throughout the animal's body. The activation signal promotes the formation of a new head whereas the inhibitory signal represses the formation of a second head near an existing head, and restricts bud formation to the lower part of the body, closer to the foot side. The position-dependent activation and inhibition activity and their propagation throughout the *Hydra* body were extensively investigated in a series of grafting experiments in which the influence of the grafted tissue was

studied as a function of the original position of the tissue in the donor animal and the grafting position in the host animal (reviewed in (22)).

During regeneration from tissue segments, following the removal of the head and foot regions, a new head organizer has to emerge. While the entire gastric tissue has the potential to form a new organizer, the realization of this potential typically occurs only in the most apical part of the excised tissue (5). Work over the last few decades has elucidated many of the molecular factors associated with organizer formation and polarity determination in *Hydra* (3, 7, 23-25). In particular, the most prominent pathway associated with the head activator is the Wnt pathway, with the expression of Wnt3 at the tip of the hypostome appearing to be one of the earliest indications for the formation of a new head organizer (3, 7, 23, 26). Perturbations that globally upregulate the Wnt pathway, for example by overexpressing a β-catenin transgene (27) or by pharmacological stabilization of β-catenin by alsterpaullone (28), have been shown to induce multiple head organizers across the entire *Hydra* body column. The Wnt pathway also appears to be activated as part of the wound healing response in excised tissues (23-25, 29). For example, following bisection, local Wnt3 concentrations have been reported to increase near the wound site at the apical side of the tissue via an apoptosis-mediated mechanism (29). While it is clear that signaling pathways are locally activated near the wound site (25), it remains unclear what discriminates between the apical and distal sides of the wounded tissue (24).

In addition to biochemical signals involved in *Hydra* polarity, there is some evidence suggesting that structural factors can also play a role in the formation of a new head organizer. Early work indicated that the local structure (30) and the shape of the closure region of the apical injury site (5) can affect the potential for head formation. More recently, we found that the cytoskeletal organization has a major influence on body axis formation during regeneration from excised tissue pieces (31, 32). We showed that the parallel array of ectodermal supra-cellular actin fibers in the parent animal remains partially intact in excised tissue segments, providing a structural memory of the alignment of the body axis in the parent *Hydra* that defines the alignment of the body axis in the regenerating animal (31). In subsequent work, we showed that local defects in the organization of these actin fibers act as organization centers for morphogenesis, with morphological features appearing at defect sites (32). In particular, we showed that the head formation in regenerating tissue fragments occurred at the site of an aster-like defect in the alignment of the ectodermal actin fibers (known as a +1 nematic topological defect).

Despite this progress, the mechanisms involved in the memory of polarity and the establishment of a new organizer in regenerating *Hydra* are still unclear. Here we combine classic experimental design with modern imaging techniques to gain insight into this important process. We study the regeneration of composite tissues generated by careful adhesion of two excised tissue rings in configurations in which the rings' polarities are not mutually aligned and/or their relative positions along the original body axis are rearranged. As such, our experiments are designed to introduce frustration in the biochemical and structural factors associated with body axis polarity, so the polarity of the fused ring doublets cannot be simply defined by the original polarity of the excised tissues. We follow the regeneration dynamics and cytoskeletal organization of the composite ring doublets by live microscopy and find that they display higher flexibility to reorganize their body axis compared to bisected animals (that retain either a head

or a foot and maintain their original polarity). This allows us to expose the plasticity of body axis polarity in *Hydra*, and identify different factors that influence polarity determination.

We find that under certain frustrating configurations, the original tissue polarity can be reversed, with a head regenerating from the most distal part of one of the excised rings, on its originally foot-facing edge. Such polarity reversal is not compatible with models assuming that the body axis polarity is determined based solely on preexisting morphogenetic gradients in the excised tissue. Rather, our experiments reveal the ability of tissue polarity to rearrange dynamically after resetting its previous memory to accommodate the imposed initial and boundary conditions. Furthermore, our results illustrate the importance of mechanical processes and cytoskeletal organization towards the establishment of polarity in the regenerated animal, consistent with our recent observations (31, 32). These results complement the large body of classical work on polarity in *Hydra*, and allow us to offer a dynamic view of polarity determination during regeneration, which relies on the interplay between signaling processes that are influenced by the original polarity and position of the excised tissue and mechanical processes that depend on cytoskeletal organization and the tissue architecture (33).

Results

Regeneration under frustrating conditions depends on tissue structure and polarity memory

Excised *Hydra* tissue rings retain a strong memory of their original polarity, regenerating a head on their original head-side and a foot on their original foot-side (5). We have confirmed these previous observations by studying excised *Hydra* tissue rings regenerating on a wire (31) that marks their original orientation, and found that nearly all regenerated *Hydra* maintained their polarity (60 out of 61; Fig. S1). In these experiments, the polarity memory is inherited in a straightforward manner- the region that was closest to the head in the original tissue is at the site of the healed wound on one edge of the tissue and develops into the head of the regenerated animal, whereas the region closest to the foot in the original tissue, at the opposite edge, becomes the foot.

To explore the interplay between polarity memory and structure we set out to generate frustrating initial configurations in which the tissue polarity cannot be maintained in a simple way. This is achieved by fusing two rings (excised from separate animals) along their axis to form a single composite tissue. The configuration of the composite ring doublet can be modulated in a controlled manner by varying the relative polarity of the rings and their original positions along the parent body axis (Methods). In the Head-to-Head (H2H) configuration, the two rings are placed opposing each other so the originally head-facing sides of the two rings adhere (Fig. 1A). To realize this, the excised rings are threaded on a wire (31, 34) in opposing orientations, maintained there for ~6 hours to allow the tissues to adhere, and subsequently removed from the wire and followed by time lapse microscopy (Methods). Whereas the polarity signals in the H2H configuration favor head formation at the middle, the structure of the fused ring doublet resembles that of a (single) thicker ring in which the open ends seal and a head regenerates at one edge. To enable tracking of the tissue dynamics in the fused ring doublets, the original animals were differentially marked by electroporating distinct fluorescent cytosolic dyes (Methods).

The majority of fused ring doublets in the H2H configuration were able to regenerate and form a head (i.e. a hypostome with two or more tentacles) (145 out of 164 samples). The outcome morphologies of the regenerated animals were diverse (Figs. 1B, S2). More than half (85/145) of the regenerated ring doublets formed a head in the middle, as expected based on the original tissue polarity (Fig. 1C, S2ii,iii; Movie 1). Yet more than 30% of the samples (45/145) formed a head on one of the sides of the ring doublet (Fig. 1D; Movie 2), i.e. at a site that was originally a foot-facing side of one of the fused rings. Occasionally, the regenerating animals formed both a head in the middle and on the side (11/145; Figs. 1B, S2v). Our results indicate that, surprisingly, regenerating *Hydra* can form a head at the distal end of the tissue, i.e. at the region that was farthest from the head in the parent animals.

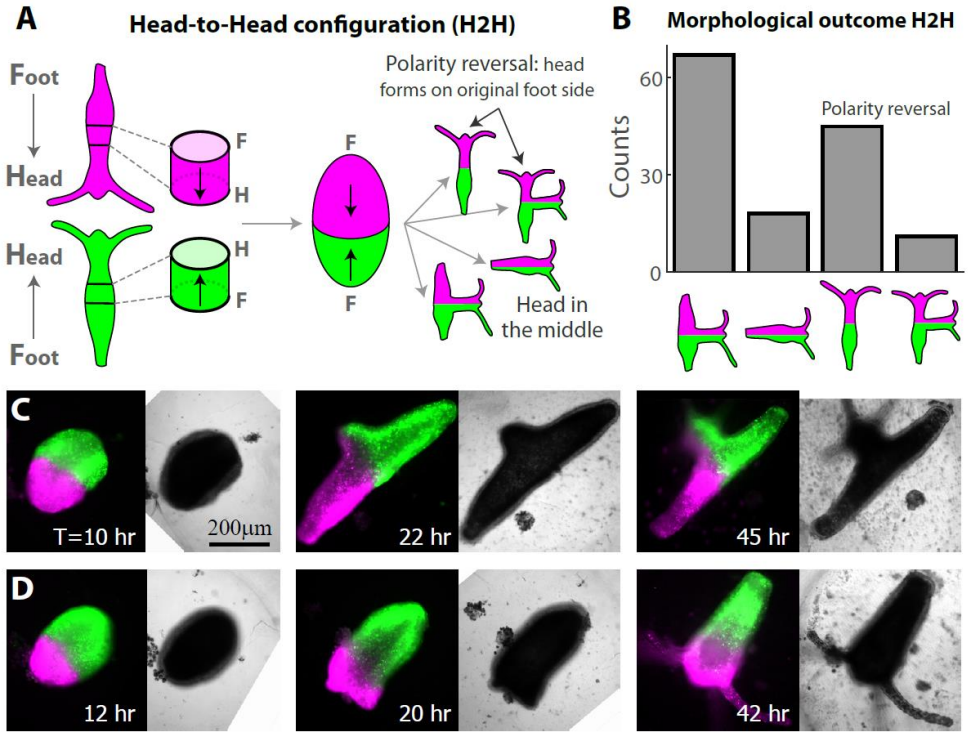

Fig 1- Polarity rearrangement in regenerating Head-to-Head (H2H) ring doublets. (A) Schematic illustration of the regeneration experiments with fused ring doublets in the H2H configuration. Two rings are excised from different animals (labeled in green or magenta). The rings adhere to each other at their head-facing sides, and the regeneration of the fused ring doublet is followed over time. (B) Bar plot depicting the outcome morphologies of fused H2H ring doublets. Experiments were performed on 164 samples. 2/164 disintegrated, 17/164 did not regenerate, and 145/164 regenerated. (C) Images from a time lapse movie of a H2H doublet that regenerated into an animal with a head in the middle (Movie 1). (D) Images from a time lapse movie of a H2H doublet that underwent polarity reversal, regenerating into a normal morphology with a head developing from an originally foot-facing side of one of the excised rings (Movie 2). The panels in (C,D) depict combined epifluorescence (Left; green- AlexaFluor 647-conjugated 10kD dextran, magenta- Texas Red-conjugated 3kD dextran) and bright-field (Right) images at the specified time points during the regeneration (time after excision in hours).

The lack of head formation at the middle in a considerable fraction of the H2H samples (Fig. 1B,D), suggests that the presence of the second ring has a repressing effect on head formation. To examine the influence of the interface between the two rings on head formation, we designed experiments in which we purposefully added a physical perturbation at the adhesion interface by placing a 75 μm-wide wire at the fusion interface for ~6 hours (Fig. S3C; Methods). The transient introduction of this perturbation at the interface reduced the fraction of samples that fail to preserve their original polarity, with the vast majority of samples growing a head in the middle of the composite tissue (Fig. S3D). The increase in the fraction of ring doublets that form a head at the interface following this transient perturbation (86% = 24/28, compared to 66%=96/145 without a wire), is aligned with earlier observations by Shimizu and Sawada that showed that structural abnormalities at the graft site correlated with additional head formation in tissue transplantation experiments in mature *Hydra* (30).

The influence of the original tissue position on polarity determination

The potential to regenerate a head and form a new organizer is present in the entire gastric tissue in *Hydra*. Yet, the head activation potential appears to be graded along the body axis, decaying away from the head organizer (35). This is illustrated by classic grafting experiments which demonstrate that the probability to form a new head increases when the source of the grafted tissue is closer to the head of the donor animal (22, 36). The graded head activation potential is also reflected in the time it takes to regenerate a head, which increases if the site of decapitation is further down the body column (17, 37). The position-dependent variation in the regeneration potential of *Hydra* tissues was further demonstrated by experiments by Sugiyama and coworkers who formed elongated cylindrical tubes by fusing a large number of tissue rings, and showed that the potential to form head structures depended on the original location of the excised rings along the body axis of the parent animal (34). We therefore ask: What are the implications of the graded head activation potential in the parent animals on the plasticity and reorganization dynamics of polarity in regenerating tissues?

The regeneration outcome in the H2H configuration reflects a competition between the memory of the original tissue polarity, and the structure imposed by the fusion of the two rings to each other. This competition masks the influence of the position of the excised tissue in the parent animals (Fig. S3). To focus on the effect of the original tissue position, we turned to ring doublets in the Head-to-Foot (H2F) configuration, maintaining the ring polarity in the same orientation by adhering the originally head facing side of one ring to the originally foot-facing side of the second ring, while varying the original positions of the rings in the parent animals (Fig. 2A). The rings are excised from different tissue locations by bisecting a *Hydra* in the middle and taking either the **U**pper ring (above the midline; **U**) or the **L**ower ring (below the midline; **L**) (Fig. 2A; Methods). The ring doublets are then fused in the H2F configuration, in an *oriented* manner that maintains their relative positions along the body axis (Fig. 2A top), or in an *anti-oriented* manner with the upper ring positioned below the lower ring (Fig. 2A bottom). Note that in both orientations, the first ring faces an additional ring on its apical interface, while the second ring has a free edge on its apical side. Importantly, while in the H2H configuration the two rings have opposite initial polarities, in the H2F configuration the fused doublet has a "preferred polarity" along which it can regenerate while maintaining the original polarity of both rings.

The regeneration of H2F ring doublets was found to dramatically depend on the relative tissue positions of the excised rings in the parent animals (Fig. 2). The regeneration of ring doublets that were fused in an oriented manner, preserving both the polarity and the relative position of the excised rings along the body axis, invariably resulted in normal animals, with a head regenerating on the original head-facing side (the U side) at one end of the doublet and a foot forming on the original foot-facing side at the other edge (the L side; Fig. 2B top, 2C; Movie 3). Note that none of the samples developed a head in the middle, despite the presence of an originally head-facing tissue there, illustrating again (as in the H2H configuration) the repressing effect of additional tissue at an originally-apical interface (Fig. 2F).

Ring doublets that were fused in an anti-oriented manner displayed markedly different behavior, with variable morphological outcomes and a high incidence of polarity reversal (Fig.

2B bottom). Only about a third of the regenerated samples (25/72) developed a normal morphology along the direction of the original body axis, whereas a considerable fraction (17/72) of samples formed a head on the foot-facing side of the upper ring, thus regenerating into an animal with a polarity that is *flipped* relative to the original body axis of both rings (Fig. 2D; Movie 4). In both of these cases, the regenerated animal has a normal morphology, either along the original polarity of the excised rings or in the opposite orientation. In other cases, as in the H2H configuration, the frustration caused by the presence of the second ring and the competition between different sites, is resolved by alternative configurations with a head in the middle (19/72) or two heads (9/72; Fig. 2D).

These results highlight the influence of the original tissue position along the body axis of the parent animal as an important factor, in addition to the original polarity and structure of the regenerating tissue, in determining the polarity of the regenerated animal. The naively expected regeneration trajectory in the H2F configuration is the formation of an animal that preserves the original polarity in both rings, developing a head at the free edge of an originally head-facing side. This is indeed the case in the H2F oriented configuration; the original polarity is maintained in nearly all the samples. In contrast, the majority of the H2F anti-oriented samples do not follow this trajectory, revealing the importance of the original position of the tissue along the body axis of the parent animal in the processes involved in polarity determination. In some cases, as in the H2H configuration, the structural repression of a head in the middle is not strong enough and the frustration is resolved by forming a head in the middle (as a single head or in addition to a head at the edge). The truly unexpected result is the anti-oriented samples which regenerate into a normal morphology with a flipped polarity (Fig. 2D); despite having a free head-facing edge, these samples regenerate by growing a head on the opposite side, on an originally-foot facing edge. This exposes a dynamic aspect of the establishment of polarity that was not appreciated before, involving an interplay between position-dependent regeneration kinetics and structural factors that jointly lead to this surprising outcome in a large fraction of the samples.

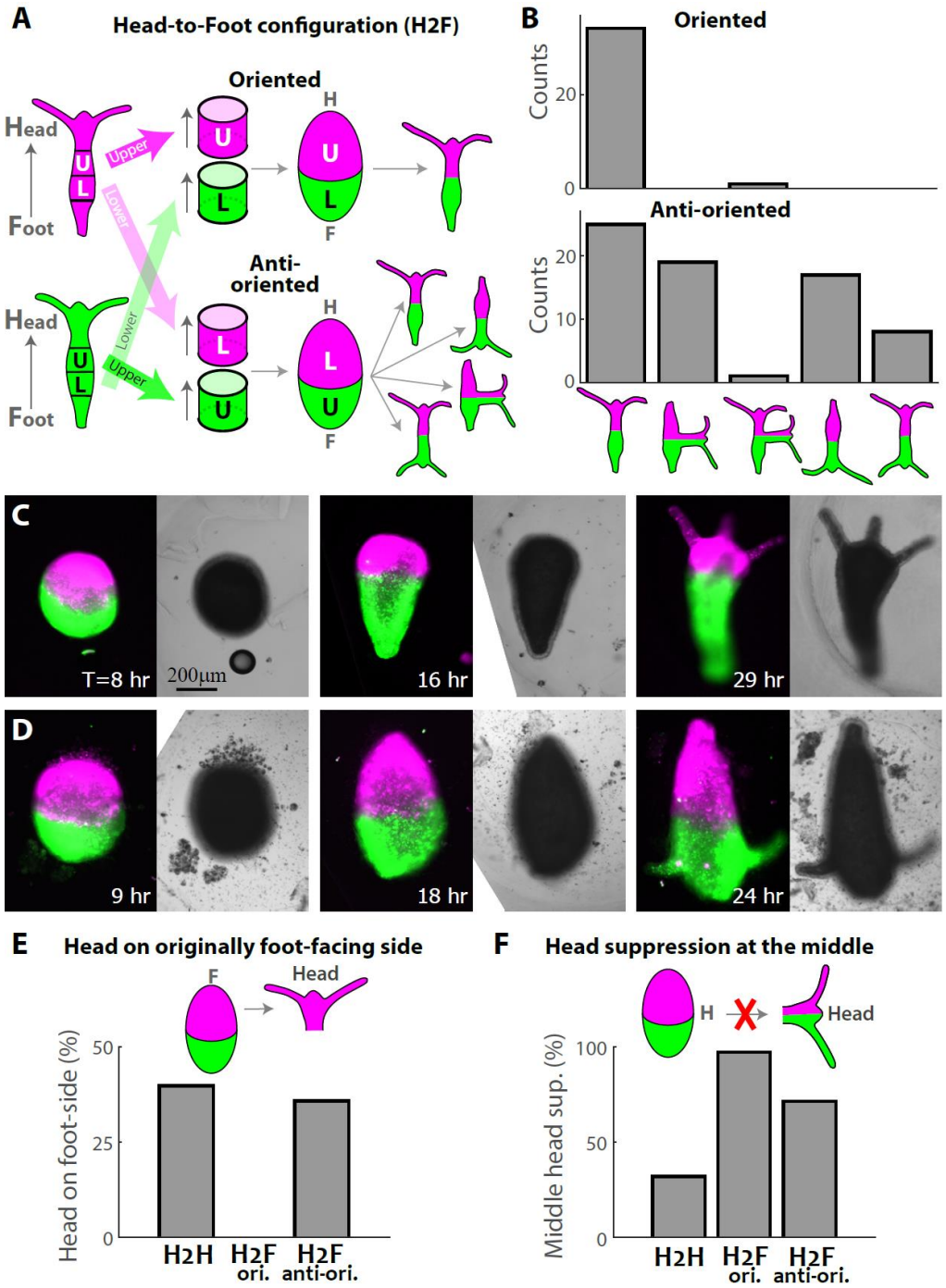

Figure 2 – Regeneration of Head-to-Foot (H2F) ring doublets depends on the original position of the excised rings within the parent animals. (A) Schematic illustration of the regeneration experiments with fused ring doublets in the H2F configuration. Rings are excised from above (**U**) or below (**L**) the approximated midpoint of the two parent animals that are differentially labeled (green/magenta). The rings are fused so that the head-facing side of the first ring adheres to the foot-facing side of the second ring in an oriented configuration that preserves the relative position of the rings (top) or an anti-oriented manner (bottom). (B) Bar plot depicting the outcome morphologies of fused ring doublets generated in the H2F configuration in an oriented (top) or anti-oriented manner (bottom). Experiments were

performed on 37 oriented ring doublet samples and 78 anti-oriented samples. In the oriented samples 1/37 disintegrated and 36/37 regenerated, with 34/36 regenerating along the original polarity. In the anti-oriented no samples disintegrated, 6/78 did not regenerate, and 72/78 regenerated into one of several possible outcome morphologies. (C) Images from a time lapse movie of an oriented H2F doublet that regenerated into a normal animal along the original body axis orientation (Movie 3). (D) Images from a time lapse movie of an anti-oriented H2F doublet that regenerated into an animal whose body axis is oriented in the opposite direction to its original polarity, with a head forming on the original foot-facing side (Movie 4). The panels in (C,D) depict combined epifluorescence (Left; green- AlexaFluor 647-conjugated 10kD dextran, magenta- Texas Red-conjugated 3kD dextran) and bright-field (Right) images at the specified time points during the regeneration. (E) Bar plot summarizing the incidence of head formation on an originally foot-facing edge (polarity reversal) in regenerating ring doublets in the H2H and H2F oriented and anti-oriented configurations. (F) Bar plot summarizing the incidence of head suppression at an originally apical region in the middle of regenerating ring doublets in the different configurations. The data in (E, F) is based on Figures 1B,2B.

Position-dependent inhibition of second head formation

The formation of two heads in regenerating fused ring doublets is infrequent, even though separately the two excised rings would each regenerate a head on their apical side. The suppression of the formation of a second head occurs even in the H2F configuration, in which the composite tissue contains two distinct regions with apical-most tissues (Fig. 2B), suggesting that the formation of one head in a regenerating tissue inhibits the formation of the second head (38). To examine the inhibition of second head formation during regeneration and the factors influencing the choice of the head-forming site, we turned to ring doublets in the Foot-to-Foot configuration (F2F; Fig. 3). In this configuration, the two rings adhere on their foot-facing side, so the composite tissue has two originally head-facing sides at both ends, allowing in principle the formation of two heads at both edges of the ring doublet.

We find that the majority of F2F doublets developed into animals that have a normal morphology with a single head (37 out of 51 samples that regenerated; Fig. 3B,D; Movie 5), with a minority regenerating two heads on both sides (12/51; Fig. 3E; Movie 6). Thus, even though there is no structural barrier for head formation at both ends of the composite tissue, the formation of a second head is frequently suppressed. This inhibitory effect is consistent with previous observations of the inhibition of head formation in the vicinity of clusters of head-activating cells in regenerating aggregates (38).

To examine the position-dependent factors associated with this suppression we focused on asymmetric F2F ring doublets, combining rings from the regions above and below the midpoint (Fig. 3A). We find that head formation always occurs on the side that was originally closer to the head in the parent animals (the **U**-side; Fig. 3C). We do not observe foot formation in the middle, indicating that the presence of a second ring represses foot development, in analogy to the suppression of head formation in the middle in the H2H and H2F configurations (Fig. 2F). These results illustrate again the influence of the original tissue position along the body axis of the parent animal on head formation; of the two original apical sites at the edges of the fused ring doublet, the site that was originally closer to the head “wins” (i.e. regenerates a new head), whereas head formation at the second site is typically suppressed (Fig. 3B,C).

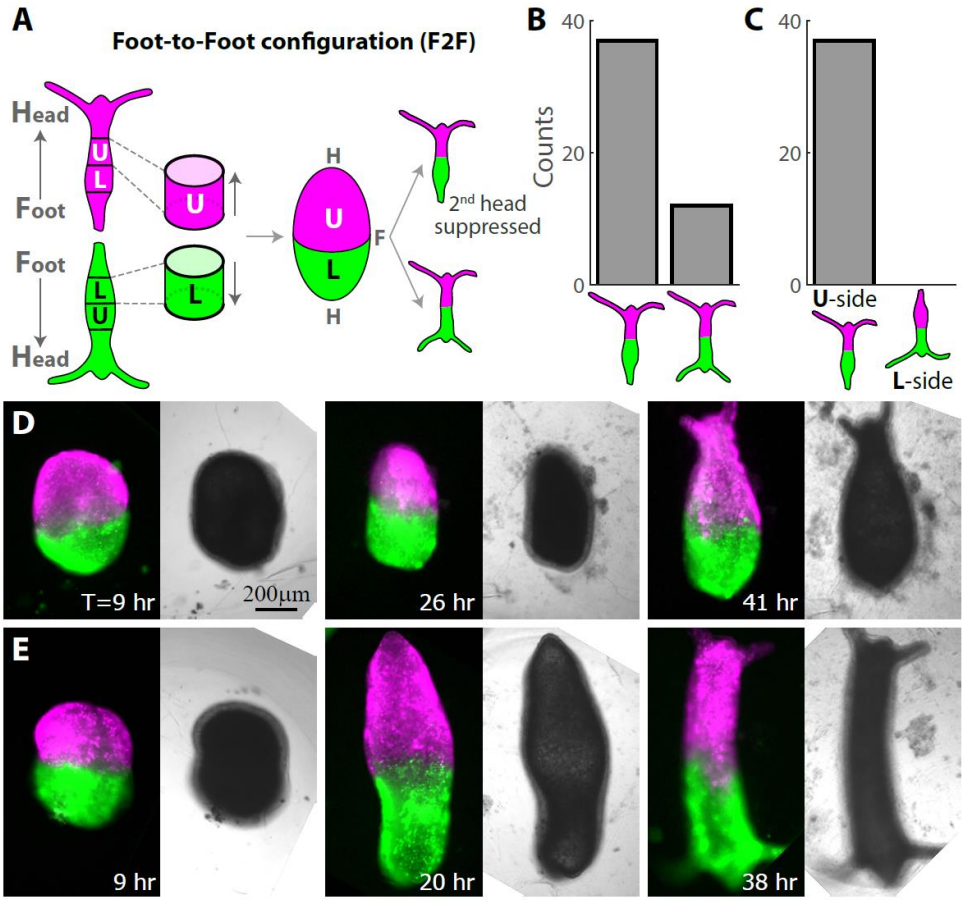

Figure 3 – Position-dependent inhibition of second head formation in regenerating Foot-to-Foot (F2F) ring doublets. (A) Schematic illustration of the regeneration experiments with fused ring doublets in the F2F configuration. Rings are excised from above (U) or below (L) the approximated midpoint of animals that are differentially labeled (green/magenta). Two rings from different positions (U and L) are fused to each other at their foot-facing sides, and the regeneration is followed over time. (B) Bar plot depicting the outcome morphologies of fused ring doublets generated in the F2F configuration. Experiments were performed on 53 samples. 1/ 53 disintegrated, 1/53 did not regenerate and 51/53 regenerated. (C) Bar plot showing the bias in head formation depending on the original position of the excised tissue rings (U or L). The original position of the excised ring on the side of the tissue where a head appeared was recorded for all F2F ring doublets that regenerated into an animal with a single head. In all these samples, invariably, the head formed on the U side. (D) Images from a time lapse movie of a F2F ring doublet that regenerated into an animal with a single head on the U side (Movie 5). (E) Images from a time lapse movie of a F2F ring doublet that regenerated into an animal with two heads on both sides (Movie 6). The panels in (D,E) depict combined epifluorescence (Left; green- Texas Red-conjugated 3kD dextran, magenta- AlexaFluor 647-conjugated 10kD dextran) and bright-field (Right) images at the specified time points during the regeneration (time after excision in hours).

Defects in the supra-cellular actin fiber organization as "attractors" for head formation

The outcome morphologies of regenerating ring doublets in the different configurations highlight the contribution of structural factors to polarity determination during regeneration. In particular, we find a bias that favors head formation at the edge of regenerating ring doublets (Fig. 2E) and tends to suppress head formation in the middle (Fig. 2F). An important feature that

distinguishes the edges of fused ring doublets from the rest of the tissue is the local organization of the supra-cellular actin myonemes. The ectodermal actin myonemes form a parallel array of supra-cellular fibers that span the entire length of a mature (31, 39). An excised tissue ring inherits this parallel actin fiber array from the parent animal (31). Single regenerating rings typically seal the top and bottom edges of the ring (unless they undergo buckling (31, 40)), to form a closed spheroid. As a tissue ring seals at its ends, the actin fibers aligned parallel to the ring's axis converge at both ends into a small region with a characteristic aster-like organization of fibers at the edges (Fig. 4A). As shown below, the edges of composite ring doublets seal in a similar manner and therefore also contain an aster-like arrangement of actin fibers.

A parallel arrangement of rod-like objects, such as the actin fibers in *Hydra*, is seen in various living and non-living systems and is referred to as a *nematic* organization (32, 41). This nematic phase has been studied extensively, e.g. to describe the behavior of liquid crystals. Mathematically, the nematic alignment of such objects is described by a director field that specifies the spatial distribution of the preferred local orientation (32, 41). Note that the director field reflects a preferred alignment but not a polarity, which is expected if the underlying constituents are apolar (i.e. rod-like objects with indistinguishable ends). In our case, even though individual actin filaments are polar, the contractile actin myonemes bundle together many actin filaments with opposite polarities and are hence expected to be apolar.

The overall parallel alignment in a nematic system can be locally distorted, forming point defects (i.e. singularities) in the director field (41). For example, at the edge of a sealed *Hydra* tissue ring, the fibers converging into an aster are not locally aligned and hence define a local point defect (Fig. 4a). Nematic point defects can be characterized by a "topological charge", or winding number, which is the number of times the director denoting the fibers' orientation rotates around the center of the defect (41). Similar to electrical charge, the total nematic topological charge in a closed system is conserved. Moreover, the total charge on a closed spheroid is constrained by topology to be equal to +2 (41). According to this nomenclature, the aster-like defects found at both ends of a sealed tissue ring, each have a topological charge of +1 (since the director field completes a full rotation around the defect), summing up to a total charge of +2 in the closed tissue spheroid as required. Similarly, in the mature *Hydra,* two +1 defects are located at the tips of the mouth and foot (32).

Since polarity in individual regenerating rings is preserved, the regions around the +1 defects at the edges of the originally head or foot facing-side of an excised ring, should develop, respectively, into the head or foot of the regenerated animal (Fig. 4A). To directly demonstrate this, we follow the actin organization in regenerating tissue rings expressing lifeact-GFP that labels the actin filaments in the ectoderm layer (31, 32, 39) and mark the apical region of the excised tissue by locally uncaging a fluorescent dye there (32) (see Methods). Indeed, we find that the edges of a sealed ring have a net topological charge of +1 (that can be localized at a point, or spread out over a small region) and that the tissue polarity is preserved with a head forming from the labeled region at the apical edge (Fig. 4B; Movie 7). In particular, the region surrounding the +1 defect at the apical edge becomes the site of the new head organizer at the tip of the mouth of the regenerated *Hydra* (Fig. 4B).

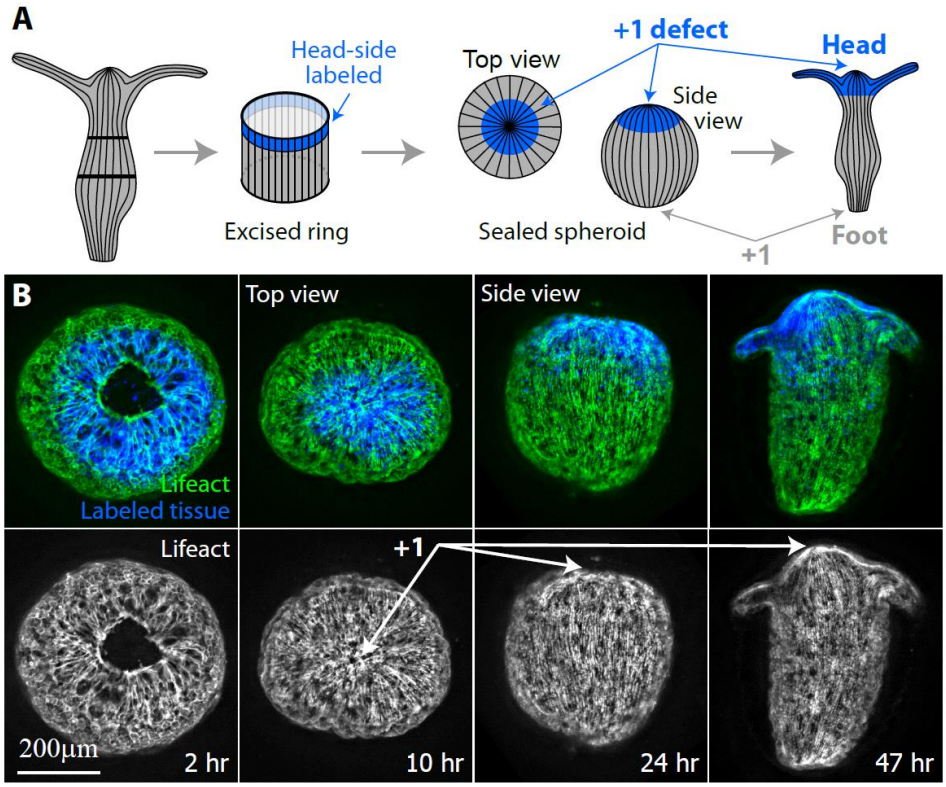

Figure 4 – Actin fiber organization in a single regenerating ring. (A) Schematic illustration of the ectodermal actin fiber organization during regeneration of an excised ring. Left: The actin fibers in a mature *Hydra* are arranged in a parallel array, along the direction of the body axis. Middle left: An excised ring inherits this actin fiber organization. The region at the apical end of the excised ring is labeled (blue). Middle right: the excised ring closes into a spheroid by sealing the open ends at its top and bottom sides. Two aster-like defects with a net topological charge of +1 (32) form at both ends of the sealed spheroid. Right: The excised ring regenerates into an animal with a new head forming at the +1 defect site located at the originally head-facing (labeled) side of the excised ring, and a new foot forming at the other end. (B) Spinning-disk confocal images from a time-lapse movie of an excised ring that is labeled at its apical end (Movie 7). The labeling is done by locally uncaging an electroporated caged-dye (Abberior CAGE 552; see Methods) (32). Images are shown at frames providing a top view of the regenerating ring from its apical end (left images) or a side view of the tissue (right images) at different time points during the regeneration process. Bottom: The projected lifeact-GFP signal (Methods) showing the organization of the ectodermal actin fibers. The +1 defect at the apical side of the sealed spheroid is clearly visible from the top view, and coincides with the site of formation of the new organizer at the tip of the hypostome of the regenerated animal. Top: Overlay of the lifeact-GFP signal (green) and the fluorescent tissue label (blue) that marks the tissue originating from the apical side of the excised ring.

How do the actin fibers organize during regeneration of fused ring doublets? We follow the dynamic organization of the ectodermal actin fibers in regenerating doublets expressing lifeact-GFP (31, 32, 39), together with fluorescent probes labeling the tissue originating from either of the fused rings in the doublet (Methods). We utilize a spinning-disk confocal microscope to image the supra-cellular ectodermal actin fibers together with the tissue marker during the regeneration process. Following fusion, the two excised rings form a composite tissue that seals in a purse-string manner at both ends, similar to a single ring. Importantly, the closure regions at

both edges of the fused doublet contain aster-like defects in the organization of the actin fibers with a net topological charge of +1 (Fig. 5).

At the adhesion interface between the two rings, the excised tissues heal in a reasonably smooth manner. In particular, ectodermal actin fibers from the two rings, aligned along the common original axis of the parent animals, can form continuous cables that bridge across the interface between the two tissues in an ordered fashion with no apparent defects (Fig. 5A,B). In some cases, the adhesion interface is not fully organized into a continuous parallel array of fibers. Nevertheless, since the fibers share the same overall orientation in the surrounding regions within the fused rings, the net topological charge at the regions near the interface between the two rings is still 0. Thus, from the point of view of the organization of the actin fibers and the topological charge of the nematic defects, the edges of the ring doublet with their associated +1 defect are clearly distinct from the middle of the fused ring doublet that has a net charge of 0.

The organizer in a mature *Hydra* is located at the tip of the hypostome which is the site of the +1 defect at the mouth (32). During regeneration following head amputation, a new organizer develops within the healed apical wound region, which invariably contains a +1 defect that forms rapidly as the wound at the edge of the amputated body column closes. Similarly, in a regenerating ring that seals at the top and bottom sides, the new head forms at the +1 defect site at the apical edge (Fig. 4). In these cases, the polarity is maintained in a straightforward manner as the new head develops at the apical wound. Since the location of the +1 defect coincides with the dominant signaling center at the apical wound healing site, it is difficult to assess the contribution of the presence of a +1 defect for head organizer formation in this configuration.

The regeneration of fused ring doublets in the presence of frustration generates conditions in which polarity cannot be trivially maintained, and therefor provides a valuable opportunity to expose the contribution of the local structure to the establishment of a new organizer. We focus on regenerating H2H doublets where the formation of a head in the middle is suppressed (and hence the original polarity is not maintained), and find that the regenerated head is always observed to emerge at the site of a preexisting +1 defect at the doublet's edge (Fig. 5A-C; Movie 8). As in a single ring, the defect characterized by a net topological charge of +1 forms rapidly (typically within ~1-3 hours) at the edge, as the parallel ectodermal fibers converge in the sealed wound. However, in this case, the tissue region surrounding the defect was farthest from the head in the parent animal. The formation of a new head at a +1 defect site at an originally distal, foot-facing edge of a ring doublet, is similarly observed during polarity reversal in the anti-oriented H2F configuration (Fig. S4). Importantly, in both of these cases in which head formation at the middle is suppressed, the alternative site at which a head appears is *not random* - head formation occurs precisely at the +1 defect site at the edge of the composite tissue (Figs. 5C, S4). In other words, under these circumstances, a preexisting +1 defect at the edge serves as an "attractor" for head formation.

The effect of structural factors on regeneration is also reflected in the suppression of head formation in the middle of ring doublets. While the apical side of individual rings invariably regenerates a head, in ring doublets where the apical side of one ring faces another tissue, head

formation is often suppressed (Fig. 2F). This is most apparent in the oriented H2F configuration, in which nearly all samples regenerate into normal animals along their original polarity and suppress head formation in the middle (Fig. 2A-C). More surprising are the cases of polarity reversal in the anti-oriented H2F configuration, in which head regeneration occurs on an originally foot-facing side of the U ring, rather than the originally head-facing side of that ring at the middle. These observations suggest that the suppression of head formation in the middle of the tissue may be at least partly related to the absence of +1 defects in the actin organization near the middle of fused ring doublets at the early stages of regeneration.

Interestingly, a head can also emerge in the middle of a fused ring doublet in a region that initially lacks defects (Fig. 5A,D; Movie 9). This is most common in H2H ring doublets where the memory of polarity introduces a strong bias for head formation in the middle (Fig. 1). In cases where this bias results in middle head formation, the emergence of a head is accompanied by reorganization of the actin fibers that involves the *de-novo* formation of defects in the actin fibers (Fig. 5D). This likely involves biochemical signaling that drives the mechanical processes leading to tissue deformations and reorganization of the cytoskeleton that results in the creation of defects in the actin-fiber organization, similar to what occurs during bud formation (39). The two +1 defects at the edges of the composite tissue in this case will become feet, as expected from the original polarity of the tissues.

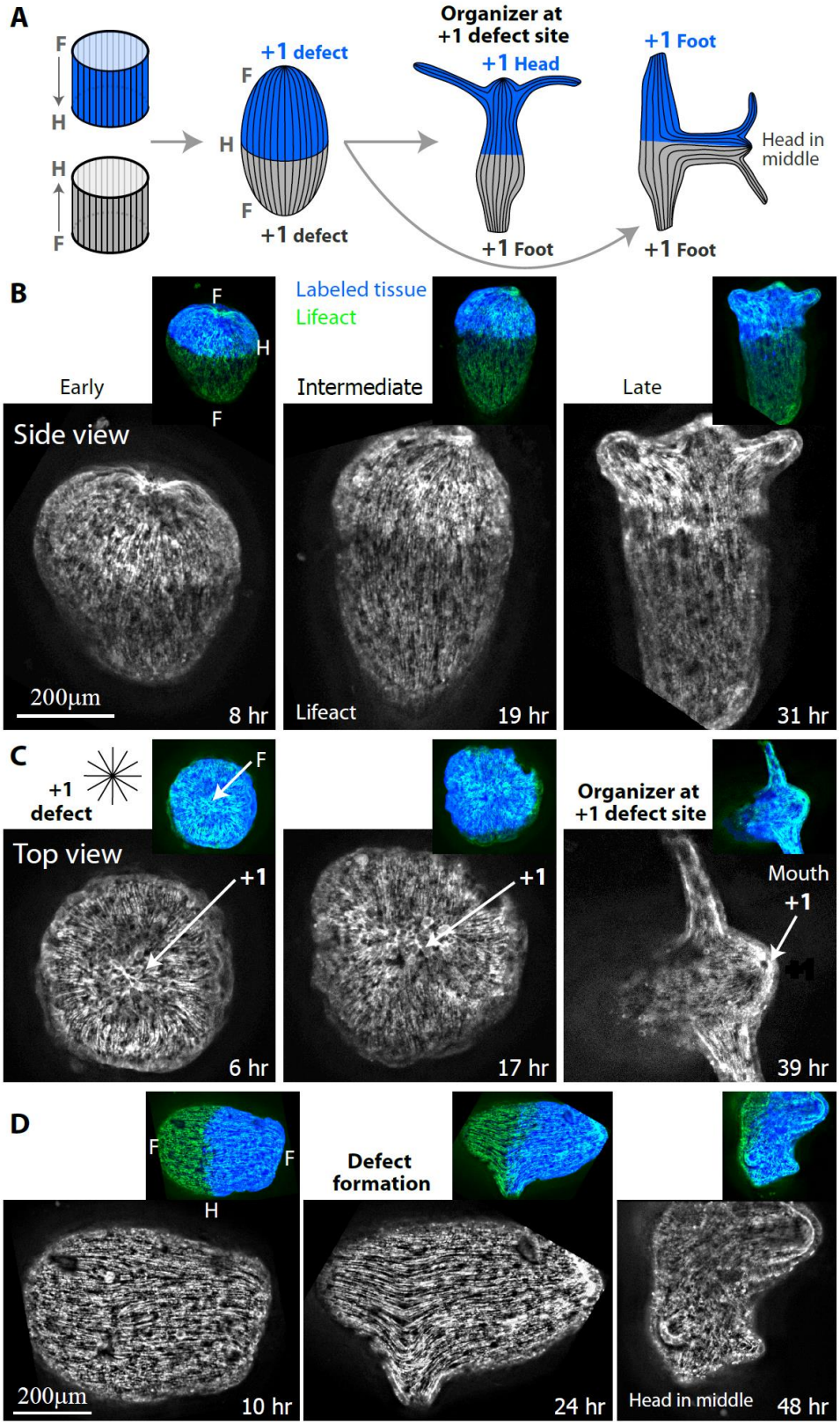

Figure 5. Actin fiber organization in regenerating H2H doublets. (A) Schematic illustration of the ectodermal actin fiber organization during regeneration of fused H2H ring doublets. Left: The actin fibers

in the excised rings are arranged in parallel arrays, along the direction of the body axis of their parent animal. The two rings are positioned in a H2H configuration, and one of the rings is marked with a fluorescent tissue label (blue). Middle: Following fusion, the actin fibers from the two rings can join to form continuous fibers that span the length of the fused ring doublet. Two aster-like defects with a net topological charge of +1 form at the top and bottom ends of the ring doublet. Right: In the case of polarity reversal (left; as in (B,C)), the fused ring doublet regenerates into an animal that has a normal morphology, with a new head forming at a +1 defect site at one edge of the doublet, and a foot forming at the other end of the doublet. Alternatively, the H2H ring doublet can regenerate a new head in the middle, according to the original polarity of the excised rings (right; as in (D)). In this case, two feet form at the +1 defects at the top and bottom ends of the fused tissue. (B,C) Spinning-disk confocal images from a time-lapse movie of a H2H doublet that underwent polarity reversal and regenerated into an animal with a head on an originally foot-facing side of one of the fused rings (Movie 8). Images are shown at frames providing a side view of the ring doublet where both rings are visible (B) or a top view of the tissue where only one ring is visible (C) at early (left), intermediate (middle) and late (right) time points during the regeneration process. The projected lifeact-GFP signal (see Methods) shows the organization of the ectodermal actin fibers. The +1 defect at the edge is clearly visible from the top view in (C), and coincides with the formation site of the new organizer at the mouth of the regenerated animal. (D) Spinning-disk confocal images from a time-lapse movie of a H2H doublet that regenerated into an animal with a head in the middle and two feet at both edges (Movie 9). The projected lifeact-GFP signal depicting the organization of the ectodermal actin fibers is shown at an early (left), intermediate (middle) and late (right) time point during the regeneration process. A +1 defect (surrounded by two -1/2 defects) forms *de novo* at the tip of a protrusion that appears at the middle of the regenerating doublet (middle) and develops into a head (right), similar to the process of bud formation (39). Insets in (B-D): Overlay depicting the lifeact-GFP signal (green) together with the fluorescent tissue label that marks one of the fused rings (blue; Texas Red-conjugated 3kD Dextran).

Discussion

While the inductive properties of an existing head organizer are evident, here we studied the process of polarity determination in excised *Hydra* tissues that initially lack a functional organizer. Given that the entire gastric tissue in *Hydra* has the potential to form a new organizer, what directs head formation to a particular site? To probe this question, we studied the reorganization of polarity in ring doublets generated in various frustrating initial configurations. Following regeneration under these conflicting circumstances exposes the dynamic nature of polarity determination, and allowed us to explore the interplay between factors associated with the original tissue polarity and position and structural factors.

The dominant view of polarity patterning in *Hydra* is based on the model developed by Gierer and Meinhardt (11, 12) (an extension of the original Turing reaction-diffusion model (10)), which assumes the existence of a relatively stable source that generates a graded distribution of a diffusible activator and an inhibitor. This model, initially developed based on phenomenological analysis of an extensive base of classic grafting experiments, has provided the main conceptual framework in the field for decades, with more recent observations related to the molecular basis of polarity determination typically interpreted within the context of this model. According to the Gierer-Meinhardt model, after removal of the head and foot regions, a regenerating tissue establishes a new organizer region by a local self-enhancing reaction that is coupled with a long-range inhibitory effect.

Importantly, the Gierer-Meinhardt model predicts that polarity will be preserved in regenerating *Hydra* tissues (12). The original inhibitory activity diminishes rapidly following the removal of the original organizer (42), so the initiation of the local activation process depends primarily on the preexisting activation properties of the tissue (sometimes termed "competence") which are graded as a function of distance from the original organizer. The molecular basis for this graded "competence" is still unclear (12), with various possibilities suggested including the distribution of signaling molecules or receptors, as well as tissue properties such as a graded enzymatic or metabolic activity level. The model assumes that the graded competence level is rather stable, and hence predicts that a new head will form at the most apical part of the original tissue and inhibit the formation of additional organizers in the tissue. We stress that the empirical support of this model is still largely lacking despite the progress in identifying the molecular players involved (12).

Our experiments challenge the current view of polarity determination. While single rings indeed regenerate according to their original polarity as expected (5) (Figs. 4,S1; Movie 7), our results with regenerating ring doublets in frustrating configurations show that tissue polarity is not always maintained (Figs. 1D,2D,5B,C; Movies 2,4,8). Furthermore, reaction-diffusion models emphasize diffusible signals as the main carriers of polarity information, overlooking the possible contribution of additional factors such as mechanical processes toward the establishment of polarity. Specifically, our observations here, further supported by recent results by us and others (32, 43), identify the importance of cytoskeletal organization at the site of organizer formation (Figs. 4,5), and suggest that tissue mechanics are an integral part of the feedback loops involved in polarity determination and stabilization. In particular, we find that head formation is biased towards the edge of the ring doublets that invariably contains a +1 defect in the organization of the actin fibers, even in cases of polarity reversal where this is opposed to the expected outcome based on the activation properties of the excised tissues (Fig. 5B,C).

Our experiments identify three factors that can have a profound impact on the polarity of the regenerating sample in a context-dependent manner: memory of the original polarity of the tissue, memory of the position of the excised tissue along the body axis of the parent animal, and constraints due to the tissue structure. While the influence of each of these factors on head regeneration on its own has already been noted in previous research (e.g. in (5) with respect to polarity memory, in (34) with respect to position, and in (30) with respect to structure), we were able to realize frustrating conditions in which these different factors cannot be simultaneously satisfied and compete with each other. Our experimental setup enabled us then to show that the interplay between these different factors can lead to surprising regeneration outcomes. Most notable in this respect are our observations of polarity reversal in the H2F configuration, in which a head grows from the region that was most distal in the excised tissue and the entire tissue regenerates with a flipped polarity (Fig. 2D; Movie 4). Note that unlike previously studied cases of polarity reversal, where the change in tissue polarity was induced externally by grafting an existing head organizer (19, 20, 44) or by exposing the tissue to a high concentration of Wnt (21) (and hence can be accommodated within the Gierer-Meinhardt model (12)), in our experiments the memory of polarity in the composite ring doublet is lost due to spontaneous internal reorganization processes.

The likely way in which these different factors combine to determine the polarity of the regenerated animal is through their influence on the kinetics of the head formation process. Once a head organizer forms in a particular region, it will suppress additional head formation in its vicinity and dominate the patterning process (38). As such, subtle differences in the kinetics at the early steps involved in head regeneration, which can be sensitive e.g. to the history of the tissue (i.e. the original polarity or the position of the excised tissue) or the local tissue structure, will be sufficient to direct head formation to a particular region and thus steer the polarity of the regenerated animal. In other words, head formation reflects a dynamic competition between different tissue regions that have the potential to support the development of a head organizer, rather than a preset biochemical patterning process that specifies a particular site. Such a dynamic view of the regeneration process can rationalize the cohort of our experimental observations in the different configurations studied, and is also consistent with previous experiments on polarity reorganization. Importantly, this dynamic view emphasizes the plasticity of the regeneration process, whereby a multi-faceted integration of multiple factors, rather than a direct causal relation, determines the polarity of the regenerated animal.

In this respect, it is important to appreciate the difference between regeneration from bisected animals (where the tissue retains either the head organizer or the foot signaling center, and hence the body axis polarity is essentially predefined) and regeneration from excised gastric tissues after removal of both the head and the foot regions. While bisection experiments are easier to perform and analyze, regeneration from excised gastric tissues provides a more sensitive platform to study axial patterning and explore how a new body axis is established (5, 31). The methodology developed here to study regeneration under frustrating conditions in ring doublets further facilitates the investigation of subtle differences in the dynamic processes involved in body axis formation, and hence should also prove useful in future research on *Hydra* polarity.

Our results also suggest some self-scaling along the body axis of adult *Hydra*, capable of setting a common scale among different animals despite the presence of inherent variation in size and signaling levels within a population, which is far from being trivial. This is evident in the striking difference between the oriented and anti-oriented H2F configuration (Fig. 2B) or in the F2F doublet configuration where we observe a complete bias for head-formation on the U-side (Fig. 3C). In both cases, the fused rings are excised from two different animals, and the relative position of the rings along the body axis of the parent animals can only be estimated rather crudely (the animal is cut approximately at the middle, but there are no special features marking the midpoint), yet the regeneration outcomes depend on the relative position of the rings within the parent animals in a consistent manner.

The onset of regeneration following excision involves an injury response (23). Injury has been shown to promote head regeneration in regeneration-deficient *Hydra* strains (45, 46), whereas the lack of injury in animals that were carefully bisected without wounding by ligature slowed down head regeneration (47). More recent experiments at the molecular level, revealed the extensive enhancement of signaling events induced by injury (23-25, 29), and further suggested that there is a different response at the apical and the distal wound that arises rapidly after injury (29). While the influence of the injury and how the tissue heals following injury is undoubtedly important for head regeneration, our results are not consistent with a model in

which injury activates head formation in a context and position-independent manner (25). Rather, we observe a position and structure-dependent bias in head formation (Figs. 1-3), indicating that the early steps in head regeneration at the site of injury must be sensitive to the history of the tissue and its local structure. Due to the effective competition between different potential sites for head formation, these local differences may be subtle, yet their effect on the regeneration outcome is nonetheless apparent.

Our experiments indicate that head formation occurs preferably (but not exclusively) at the edge of fused ring doublets, which is the site of an aster-shaped +1 defect in the actin-fiber nematic organization. Strikingly, this is true even when polarity is reversed, i.e. when a head forms at the originally foot-facing side of one of the fused tissue rings (Fig. 2E). The observed bias favoring head formation at sites of +1 defects in regenerating ring doublets, is well-aligned with recent results from our lab, which examined the role of topological defects in the actin nematic order in regeneration of tissue segments (32). In that work we showed that a +1 defect in the organization of the supra-cellular actin fibers arises in regenerating tissue fragments, and can act as an organization center for head formation. The inherent structure of +1 defects as the focal point of an aster of contractile actin fibers implies that these sites are mechanically unique (32). Moreover, once formed, +1 defects in the actin organization were shown to remain stationary relative to the underlying cells (32). As such, the cells near the core of a +1 defect experience a sustained distinct mechanical environment that can locally activate signaling pathways, effectively turning this site into an attractor for head formation. The special role assigned to +1 defects in the head formation process, is aligned with recent observations in regenerating jellyfish where the establishment of mouth structures was shown to occur at +1 defect sites (referred to as “hubs”) (43). Interestingly, they also observed local activation of the Wnt pathway specifically at the defects sites (43).

A central feature of the Grier-Meinhardt model is the autocatalytic nature of the local activation. While the Wnt pathway has been shown to be self-activated (26), we propose that the mechanical environment in the vicinity of a +1 defect can also provide sustained local activation and participate in the feedback loop. These different sources of local activation can then initiate head formation via one of two possible scenarios. In the first scenario, autocatalytic signaling events initiate head formation by creating the necessary cytoskeletal organization and mechanical conditions, as in bud formation (39) or middle-head formation in the H2H configuration (Fig. 5D). In the second scenario, the presence of a preexisting +1 defect creates a favorable site where local mechanical cues promote the activation of the necessary signaling pathways. The second scenario is the likely path that leads to head formation at +1 defect sites identified early during polarity reversal in regenerating ring doublets (Figs. 5B,C, S4, Movie 8) or in regenerating tissue fragments (32). Since the establishment of a head organizer involves a competition between different potential sites, the presence of a +1 defect does not necessarily lead to head formation. Thus, while the *Hydra* head organizer invariably contains a +1 defect, there is no simple causal relation between the presence of a +1 defect and head formation; a +1 defect is neither a prerequisite nor necessarily associated with head formation. Furthermore, as the site of a +1 defect at the edge of a ring doublet is also a region of wound healing, at this stage it is impossible to identify a cause-effect cycle between activated wound healing signaling

and mechanical cues. Nonetheless, the integration of these biochemical and mechanical processes leads eventually to a functional organizer and head formation (33).

It is noteworthy to also consider the idea of a mechanical feedback associated with the presence of a +1 defect, in relation to the question of how the stability of the head organizer in a mature *Hydra* is maintained in the presence of continuous tissue renewal (6). Earlier work has shown that all cells in *Hydra* turn over, with cell removal occurring at tip of the hypostome, the tip of the tentacles and the peduncle at the foot (48). We can now identify all these sites of cell extrusion in the mature *Hydra* as +1 defects sites (32), in analogy with recent observations in epithelial sheets *in vitro* where cell extrusion was localized at defect sites (49). To maintain a stable organizer, the loss of organizer cells that are continuously sloughed off at the tip of the hypostome must be compensated by the formation of new organizer cells. How is the rate of induction of new organizer cells fine-tuned to match the rate of cell turnover that is known to be variable e.g. as a function of the feeding rate of the animals (50)? Mechanical feedback associated with the presence of a +1 defect at the core of the organizer could contribute to the stabilization of the organizer: if the induction process of organizer cells is also dependent on mechanical cues that are influenced by the distance of a cell from the +1 defect site (that is inherently controlled by the cell turnover rate), the presence of a +1 defect at the core of the organizer would provide a self-organized mechanism for stabilizing the organizer. In other words, we propose that the stability of the +1 defects at the head supports the integrity of the head organizer and through it the integrity of the *Hydra* body plan over time.

The synthesis of our results, with the large body of work on *Hydra* polarity starting from Ethel Browne more than a 100 years ago and continued by many others over the years, generates a dynamic picture of polarity determination in regenerating *Hydra*. This dynamic view extends the model proposed by Gierer and Meinhardt, by suggesting that mechanical feedback could be an important ingredient in the patterning process of regenerating *Hydra* (33). More broadly, we believe that such an integrated framework that takes into account the symbiotic interactions between the different mechanical and biochemical factors will be essential for deciphering the mechanisms responsible for polarity determination in animal morphogenesis.

Methods

Hydra Strains and Culture

Experiments are performed with a transgenic strain of *Hydra* Vulgaris (AEP) expressing lifeact-GFP in the ectoderm (51) (generously provided by Bert Hobmayer, University of Innsbruck). Animals are cultivated in *Hydra* medium (HM; 1 mM NaHCO3, 1 mM CaCl2, 0.1 mM MgCl2, 0.1 mM KCl, and 1 mM Tris-HCl, pH 7.7) at 18^{o} C. The animals are fed three times a week with live *Artemia nauplii* and rinsed after 4 hr. Experiments are initiated ~24 hr after feeding.

Fluorescent Tissue Labeling

In order to distinctly label tissue segments originating from different parent *Hydra* we fluorescently label the animals (prior to excising rings) by electroporating fluorescent cell volume dyes. Electroporation of the dye into live *Hydra* is performed using a homemade electroporation setup (32). The electroporation chamber consists of a small Teflon well, with 2 perpendicular Platinum electrodes, spaced 5 mm apart, on both sides of the well. Four *Hydra* are placed in the chamber in 20µl of *Hydra* medium supplemented with 2mM of dye (Alexa Fluor 647-conjugated 10kD Dextran or Texas Red-conjugated 3kD Dextran, both from Invitrogen). A 150 Volts electric pulse is applied for 35ms. The animals are then rinsed in *Hydra* medium and allowed to recover for ~12 hours prior to tissue excision. Unless stated otherwise, experiments involving fusion of two *Hydra* tissue rings are performed using two separate donor animals, each labeled with a different colored dye.

To label the apical region of a single excised ring we use laser photoactivation of a caged dye (Abberior CAGE 552 NHS ester) that is electroporated uniformly into mature *Hydra* and subsequently activated in the desired region, as previously described (32). The electroporation chamber consists of 2 perpendicular Platinum electrodes, spaced 2.5 mm apart. A single *Hydra* is placed in the chamber in 10µl of HM supplemented with 4mM of the caged dye. A 75 Volts electric pulse is applied for 35ms. The animal is then washed in HM and allowed to recover for several hours to 1 day prior to tissue excision. Following excision, the specific region of interest is activated by a UV laser in a LSM 710 laser scanning confocal microscope (Zeiss), using a 20× air objective (NA=0.8). Photoactivation of the caged dye is done using a 10 mW 405nm laser at 100 %. Subsequent imaging of the lifeact-GFP signal and the uncaged cytosolic label is done by spinning-disk confocal microscopy as described below. The uncaged dye remains within the cells of the photoactivated region and does not get advected or diffuses away within our experimental time window (32).

Sample Preparation

Extracting rings with known polarity with respect to parent animal

In order to investigate the influence of the original body axis polarity on the polarity of the regenerated samples, it is necessary to excise tissue rings in a manner which preserves knowledge of their original polarity. For this purpose, we use a platinum wire (diameter: 75 µm, length: ~1 cm), bent at one end to provide a directional marker. Next, we cut off one side of the animal (head or foot) and insert the straight end of the wire into the body cavity (along its axis). An additional transverse cut removes the other side of the body (foot or head, respectively), and

leaves us with a ring threaded on the wire with known polarity. To study polarity preservation in individual rings (Fig. S1), the samples are kept on the wire and transferred to a 96 well plate for imaging. The rings are excised using a scalpel equipped with a #15 blade.

Preparation of fused ring doublets

To generate samples with frustrated initial conditions, we fuse two tissue rings to each other. We use different configurations with regards to the original polarity (H2H, H2F, F2F) and the relative body positions of the two rings (UU, LL, LU, UL). We define the relative body position in the parent animal by dividing the *Hydra* body into four parts: Head, Upper (U), Lower (L) and Foot. In all experiments we use only the U and L ring sections, positioned above and below the estimated middle of the animal, respectively. The length of each tissue ring (along the animal axis) ranges from about 1/8 to 1/4 of the full animal's length.

A fused ring doublet is generated by combining two rings, excised from two separate animals that are differentially labeled by a fluorescent dye (see above). The first ring is excised from the desired position (U or L) in one *Hydra* and threaded on a wire in the desired orientation as described above. The excised ring is then transferred, while maintaining its orientation and threaded onto a vertical 75 µm-diameter platinum wire which sticks out of a petri dish that is half-filled with 2% agarose (prepared in HM) and layered with additional HM from above. The procedure is repeated with the second ring (taken from another animal) which is placed on top of the first ring (so that both rings are immersed in HM). Although close contact for a few minutes is sufficient for establishing an initial connection between the two ring tissues, significantly longer time is needed to ensure stable fusion. An additional horizontal wire is placed on top of the two rings to hold them together. We did not observe differences in the regeneration outcome as a function of the overall orientation of the ring doublet on the vertical wire (i.e. which ring was placed on the bottom or the top of the vertical wire, as long as the overall doublet configuration was maintained).

The tissue rings are left to adhere to each other for 6-8 hours on the vertical wire. Subsequently, the wires are removed, and samples consisting of two rings that have fused together form composite ring doublets. Typically, 12-24 samples are generated in one experiment. The samples are transferred into a 25-well agarose setup placed in a 50 mm glass-bottom petri dish (Fluorodish) for imaging. The wells are produced using a homemade Teflon 25-pin comb (1.5 mm diameter pins) with 2% agarose in HM. Each sample is placed in a well which is filled with HM. The tissue originating from each ring can be identified by its distinct fluorescent label (from the parent animal labeled with a different dye). This allows us to track the dynamics of the tissues originating from each of the two rings in the regenerating fused ring doublet. Using this protocol ~90% of the samples fuse successfully.

Fused ring-doublets formed with a physical barrier in the middle

To introduce a physical barrier at the interface between the two rings forming the doublet, we insert a horizontal platinum wire (diameter: 75 µm) as an obstacle between the two rings. The procedure for preparing these samples is similar to the procedure for preparing the fused ring doublets described above, except for the insertion of the horizontal wire at the fusion interface between the two rings. The horizontal wire is placed on the bottom ring, along the interface

between the rings, before placing the second ring on it. The two rings adhere to each other around the horizontal wire (on both sides), while remaining threaded on the vertical wire that holds them in place. After ~6-8 hours the wires are removed after checking carefully that the horizontal wire was indeed pinned between the two rings (by checking the sample can be lifted using this wire). The success rate of fusion with a barrier in this geometry is ~50%.

Microscopy

Time-lapse epifluorescence and bright field movies of regenerating *Hydra* are recorded on a Zeiss Axio-Observer microscope with a 5x air objective (NA= 0.25), at room temperature. Images are acquired on a charge-coupled device (CCD) camera (CoolSnap, Photometrix), and illuminated with an XCite 120Q lamp (Excelitas Technologies). Time lapse imaging begins after the ring doublets are removed from the wire (~6-8 hours after excision) and continues for 3 days at a time interval of 10-15 minutes. We use 4 channels: bright field, Lifeact-GFP, Dextran Texas Red, Dextran Alexa Fluor 647.

Time-lapse spinning-disk confocal movies are acquired on a spinning-disk confocal microscope (Intelligent Imaging Innovations) running Slidebook software. Imaging is done using laser excitation at 488 nm (lifeact-GFP), 561 nm (Texas Red) and 640 nm (Alexa-fluor 647) and appropriate emission filters at room temperature and acquired with an EM-CCD (QuantEM; Photometrix). In some cases, to reduce tissue movements and rotations, the sample is embedded in a soft gel (0.5% low melting point agarose (Sigma) prepared in HM). Time lapse movies of regenerating *Hydra* are taken using a 10× air objective (NA=0.5). Due to light scattering from the tissue, we cannot image through the entire sample so our observations are limited to the side of the tissue that is facing the objective. Spinning-disk z-stacks are acquired with a 3-5 µm interval between slices for a total of 120 µm.

Final images of the regenerated *Hydra* are taken after 3-5 days, after relaxing the animals in 2% urethane in HM for 1 minute and sandwiching them between two glass coverslips with a 200 µm spacer between them. The samples are imaged from both sides (by flipping the sample).

Analysis

The outcome morphology of regenerated ring doublet samples is determined manually based on inspection of the time-lapse movie of the regeneration process and the final images. Regeneration is defined as the formation of a head structure with tentacles within 3 days. The regenerated samples develop a variety of different morphological structures (Fig. S2). For each doublet configuration, the outcome morphologies of the different samples are divided into several categories (as indicated schematically in the respective bar plots) based on the appearance of morphological structures head (with tentacles)/foot and their position with respect to the fused ring tissues (as determined from the distribution of the labeled tissues originating from each ring). This allows us to determine if structures such as a regenerated head originate from the interface between the two rings (and are hence labeled with both colors), or from either side of the ring doublet. The tissue originating from the head or foot facing sides of the excised rings can be identified based on the distribution of the tissue labels and the knowledge of the doublet's configuration. Polarity reversal refers to situations in which a regenerated head forms on the originally foot-facing side of one of the rings. Note that this

tissue region would invariably be the site of foot formation if the ring was allowed to regenerate on its own (Fig. 4).

The organization of the supra-cellular actin fibers in the ectoderm is followed by analyzing time lapse spinning disk confocal movies of the lifeact-GFP signal in regenerating samples, in addition to the labels marking the tissue originating from the different rings. The projected images of the supra-cellular actin fibers (myonemes) in the basal layer of the ectoderm are extracted from the 3D z-stacks at each time point as described in (32).

Acknowledgments

We thank Gidi Ben Yoseph for superb technical assistance. We thank Prof. Bert Hobmayer for generously providing transgenic *Hydra* expressing lifeact-GFP. We thank Omri Wurtzel and Tom Schultheiss for valuable discussions. We thank Omri Wurtzel and Niv Ierushalmi for comments on the manuscript.

This work was supported by a grant from the European Research Council (ERC-2018-COG grant 819174) to K.K., a grant from the Israel Science Foundation (grant No. 228/17) to E.B., and a Miriam and Aaron Gutwirth Memorial Fellowship to Y.M.S.

References

1. Gilbert SF (2013) *Developmental Biology* (Sinauer Associates, Inc.).
2. Gierer A, Berking S, Bode H, David CN, Flick K, Hansmann G, Schaller CH, & Trenkner E (1972) *Nature/New Biology***,** 98-101.
3. Hobmayer B, Rentzsch F, Kuhn K, Happel CM, von Laue CC, Snyder P, Rothbacher U, & Holstein TW (2000) *Nature* **407,** 186-189.
4. Gurley KA, Rink JC, & Alvarado AS (2008) *Science* **319,** 323-327.
5. Javois LC, Bode PM, & Bode HR (1988) *Developmental biology* **129,** 390-399.
6. Bode HR (2012) *Int. J. Dev. Biol.* **56,** 473-478.
7. Lengfeld T, Watanabe H, Simakov O, Lindgens D, Gee L, Law L, Schmidt HA, Özbek S, Bode H, & Holstein TW (2009) *Developmental Biology* **330** 186–199.
8. Alvarado AS (2012) *BMC Biology* **10,** 88.
9. Browne EN (1909) *J Exp Zool* **7,** 1-24.
10. Turing AM (1952) *Philosophical Transactions of the Royal Society of London. Series B, Biological Sciences* **237,** 37-72.
11. Gierer A & Meinhardt H (1972) *Kybernetik* **12,** 30-39.
12. Meinhardt H (2012) *Int. J. Dev. Biol.* **56,** 447-462.
13. Wolpert L, Clarke MRB, & Hornbruch A (1972) *Nature* **239,** 101-105.
14. Wolpert L (1969) *J. Theoret. Biol.* **25,** 1-47.
15. Wolpert L, Hornbruch A, & Clarke MRB (1974) *American Zoologist* **14,** 647-663.
16. Trembley A (1744) *Mémoires pour servir à l'histoire d'un genre de polypes d'eau douce, à bras en forme de cornes* (Jean & Herman Verbeek, Leiden).
17. Javois LC, Wood RD, & Bode HR (1986) *Developmental biology* **117,** 607-618.
18. Zamaraev VN (1956) *Bulletin of Experimental Biology and Medicine* **42,** 1051-1053.
19. Wilby OK & Webster G (1970) *Journal of embryology and experimental morphology* **24,** 595-613.
20. Marcum BA, Campbell RD, & Romero J (1977) *Science***,** 771-773.
21. Wang R, Steele R, & Collins E-M (2020) *Developmental Biology* **467,** 88-94.
22. Shimizu H (2012) *Int. J. Dev. Biol.* **56,** 463-472.
23. Petersen HO, Hø̈ger SK, Looso M, Lengfeld T, Kuhn A, Warnken U, Nishimiya-Fujisawa C, Schnø̈lzer M, Krü̈ger M, Ozbek S*, et al.* (2015) *Molecular biology and evolution* **32,** 1928-1947.
24. Gufler S, Artes B, Bielen H, Krainer I, Eder MK, Falschlunger J, Bollmann A, Ostermann T, Valovka T, Hartl M*, et al.* (2018) *Developmental Biology* **433,** 310-323.
25. Cazet JF & Juliano CE (2020) *bioRxiv*.
26. Nakamura Y, Tsiairis CD, Ozbek S, & Holstein TW (2011) *PNAS* **108,** 9137-9142.
27. Gee L, Hartig J, Law L, Wittlieb J, Khalturin K, Bosch TCG, & Bode HR (2010) *Developmental Biology* **340,** 116–124.
28. Broun M, Gee L, Reinhardt B, & Bode HR (2005) *Development* **132,** 2907-2916.
29. Chera S, Ghila L, Dobretz K, Wenger Y, Bauer C, Buzgariu W, Martinou J-C, & Galliot B (2009) *Developmental cell* **17,** 279-289.
30. Shimizu H & Sawada Y (1987) *Developmental Biology* **122,** 113-119.
31. Livshits A, Shani-Zerbib L, Maroudas-Sacks Y, Braun E, & Keren K (2017) *Cell Reports* **18,** 1410-1421.
32. Maroudas-Sacks Y, Garion L, Shani-Zerbib L, Livshits A, Braun E, & Keren K (2020) *Nature Physics*.
33. Braun E & Keren K (2018) *BioEssays* **40,** 1700204.

34. Ando H, Sawada Y, Shimizu H, & Sugiyama T (1989) *Developmental Biology* **133,** 405-414.
35. Bode HR (2009) *Cold Spring Harbor Perspectives in Biology* **a000463,** 1.
36. Takano J & Sugiyama T (1983) *Development* **78,** 141-168.
37. Webster G & Wolpert L (1966) *Development* **16,** 91-104.
38. Technau U, von Laue CC, Rentzsch F, Luft S, Hobmayer B, Bode HR, & Holstein TW (2000) *PNAS* **97,** 12127–12131.
39. Aufschnaiter R, Wedlich-Soldner R, Zhang X, & Hobmayer B (2017) *Biology Open* **6,** 1137-1148.
40. Krahe M, Wenzel I, Lin KN, Fischer J, Goldmann J, Kastner M, & Futterer C (2013) *New Journal of Physics* **15,** 035004.
41. Kleman M & Laverntovich OD (2007) *Soft matter physics: an introduction* (Springer Science & Business Media).
42. MacWilliams HK (1983) *Developmental biology* **96,** 217-238.
43. Sinigaglia C, Peron S, Eichelbrenner J, Chevalier S, Steger J, Barreau C, Houliston E, & Leclere L (2020) *Elife* **9,** e54868.
44. Wilby OK & Webster G (1970) *Journal of embryology and experimental morphology* **24,** 583-593.
45. MacWilliams HK (1983) *Developmental biology* **96,** 239-257.
46. Kobatake E & Sugiyama T (1989) *Development* **105,** 521-528.
47. Newman SA (1974) *Development* **31,** 541-555.
48. Campbell RD (1967) *Journal of Morphology* **121,** 19-28.
49. Saw TB, Doostmohammadi A, Nier V, Kocgozlu L, Thampi S, Toyama Y, Marcq P, Lim CT, M. Yeomans J, & Ladoux B (2017) *Topological defects in epithelia govern cell death and extrusion*.
50. Otto JJ & Campbell RD (1977) *Journal of Cell Science* **28,** 117-132.
51. Seybold A, Salvenmoser W, & Hobmayer B (2016) *Developmental biology* **412,** 148-159.

Supplementary Information

Supplementary movies

Movie 1. H2H doublet that regenerated into an animal with a head in the middle. Time-lapse movie of a H2H doublet that underwent polarity reversal, regenerating into an animal with a head in the middle and two feet at the edges. Combined epifluorescence (Left; green- AlexaFluor 647-conjugated 10kD dextran, magenta- Texas Red-conjugated 3kD dextran) and bright-field (Right) images are shown. The elapsed time from excision is displayed (hrs:min), and the scale bar is 200 μm.

Movie 2. H2H doublet that regenerated a head on its edge. Time-lapse movie of a H2H doublet that underwent polarity reversal, regenerating into an animal with a normal morphology, with a head that developed from an originally foot-facing side of one of the excised rings. Combined epifluorescence (Left; green- AlexaFluor 647-conjugated 10kD dextran, magenta- Texas Red-conjugated 3kD dextran) and bright-field (Right) images are shown. The elapsed time from excision is displayed (hrs:min), and the scale bar is 200 μm.

Movie 3. H2F doublet in the oriented configuration that regenerated along its original polarity. Time-lapse movie of an oriented H2F doublet that regenerated into a normal animal along the original body axis orientation. Combined epifluorescence (Left; green- AlexaFluor 647-conjugated 10kD dextran, magenta- Texas Red-conjugated 3kD dextran) and bright-field (Right) images are shown. The elapsed time from excision is displayed (hrs:min), and the scale bar is 200 μm.

Movie 4. H2F doublet in the anti-oriented configuration that reversed polarity. Time-lapse movie of an anti-oriented H2F doublet that regenerated into an animal whose body axis is oriented in the opposite direction to its original polarity, with a head forming on the original foot-facing edge. Combined epifluorescence (Left; green- AlexaFluor 647-conjugated 10kD dextran, magenta- Texas Red-conjugated 3kD dextran) and bright-field (Right) images are shown. The elapsed time from excision is displayed (hrs:min), and the scale bar is 200 μm.

Movie 5. F2F doublet that regenerated into a normal morphology with a single head. Time-lapse movie of a F2F ring doublet that regenerated into an animal with a single head on the U side. Combined epifluorescence (Left; green- Texas Red-conjugated 3kD dextran, magenta-

AlexaFluor 647-conjugated 10kD dextran) and bright-field (Right) images are shown. The elapsed time from excision is displayed (hrs:min), and the scale bar is 200 µm.

Movie 6. F2F doublet that regenerated two heads. Time-lapse movie of a F2F ring doublet that regenerated into an animal with two heads on both sides. Combined epifluorescence (Left; green- Texas Red-conjugated 3kD dextran, magenta- AlexaFluor 647-conjugated 10kD dextran) and bright-field (Right) images are shown. The elapsed time from excision is displayed (hrs:min), and the scale bar is 200 µm.

Movie 7. Actin organization in a single regenerating ring. Time-lapse, spinning-disk confocal movie depicting the actin organization in a regenerating ring. The apical side of the ring was labeled with a fluorescent tissue label (by locally uncaging Abberior CAGE 552) to mark the original polarity of the tissue, which is preserved in the regeneration process. Right: projected lifeact-GFP signal showing the organization of the ectodermal actin fibers. Left: overlay of the lifeact-GFP signal (green) with the fluorescent tissue label (blue). The elapsed time from excision is displayed in hours (hrs:min), and the scale bar is 100 µm.

Movie 8. Actin organization in H2H doublet that underwent polarity reversal. Time-lapse, spinning-disk confocal movie depicting the actin organization in a H2H doublet that underwent polarity reversal and regenerated into an animal with a head on an originally foot-facing side of the labeled ring. The +1 defect at the labeled edge is clearly visible from the beginning of the movie, and coincides with the site of head formation in the regenerated animal. Right: projected lifeact-GFP signal showing the organization of the ectodermal actin fibers in the ring doublet. Left: overlay of the lifeact-GFP signal (green) with the fluorescent tissue label marking one of the rings (blue; Texas Red-conjugated 3kD dextran). The elapsed time from excision is displayed in hours (hrs:min), and the scale bar is 100 µm.

Movie 9. Actin organization in H2H doublet that regenerated a head in the middle. Time-lapse, spinning-disk confocal movie of a H2H doublet that regenerated into an animal with a head in the middle and two feet at both edges. A +1 defect (surrounded by two -1/2 defects) forms *de novo* at the tip of a protrusion that appears at the middle of the regenerating doublet and develops into a middle head. Right: images of the projected lifeact-GFP signal showing the organization of the ectodermal actin fibers in the ring doublet. Left: overlay of the lifeact-GFP signal (green) with the fluorescent tissue label marking one of the rings (blue; Texas Red-

conjugated 3kD dextran). The elapsed time from excision is displayed in hours (hrs:min), and the scale bar is 100 µm.

Supplemental Figures

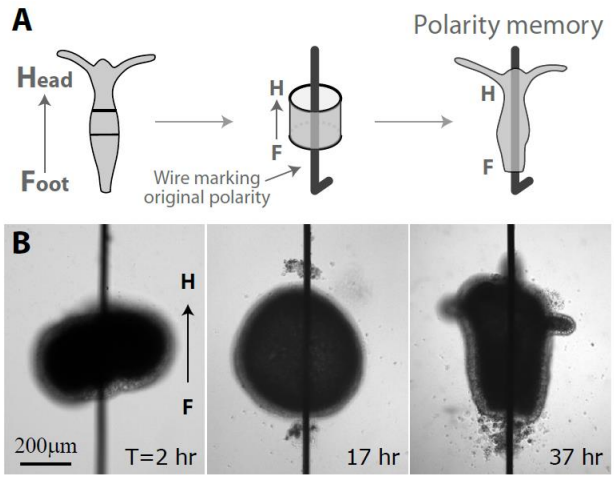

Figure S1. Memory of polarity in single tissue rings regenerating on a wire. (A) Schematic illustration of the regeneration of an excised tissue ring on a wire (31). A ring is excised from the gastric region of a mature *Hydra*. The ring is threaded on a wire that is bent at one end to mark the original polarity of the tissue. The majority of excised rings are able to regenerate on the wire (61 out of 92 samples regenerated, 12 escaped from the wire, 8 disintegrated, and 11 did not regenerate). 60 out of the 61 regenerated samples had a normal morphology that maintained the original polarity of the excised ring (1/61 samples regenerated into an abnormal morphology). (B) Images from a time lapse movie of an excised ring that regenerated on a wire. The original polarity of the excised ring is indicated, and is maintained in the regenerated animal.

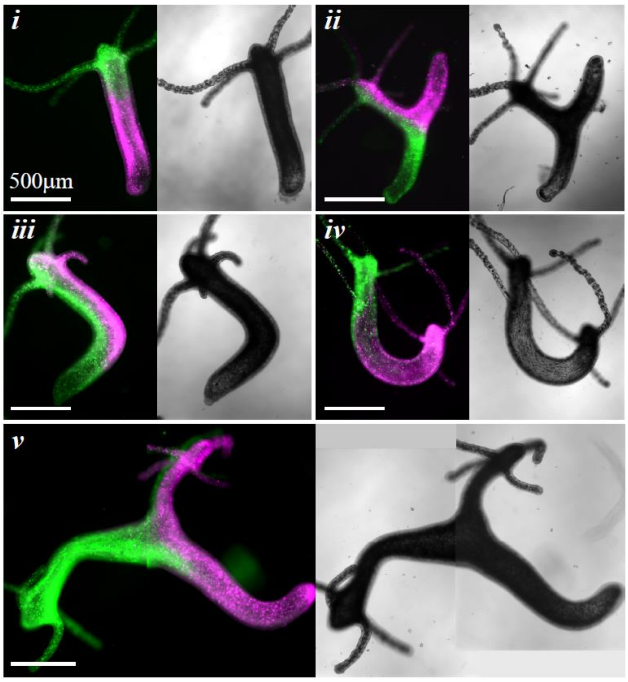

Figure S2. Different types of morphological outcomes in regenerating ring doublets. Combined epifluorescence (Left; green- AlexaFluor 647-conjugated 10kD dextran, magenta- Texas Red-conjugated 3kD dextran) and bright-field (Right) images of different outcome morphologies observed in the regeneration of ring doublets in the various configurations: (i) Normal (ii) Head in the middle with two feet (iii) Head originating from the middle of the doublet with normal morphology (iv) Two heads at opposite sides and (v) Heads in the middle and on the side.

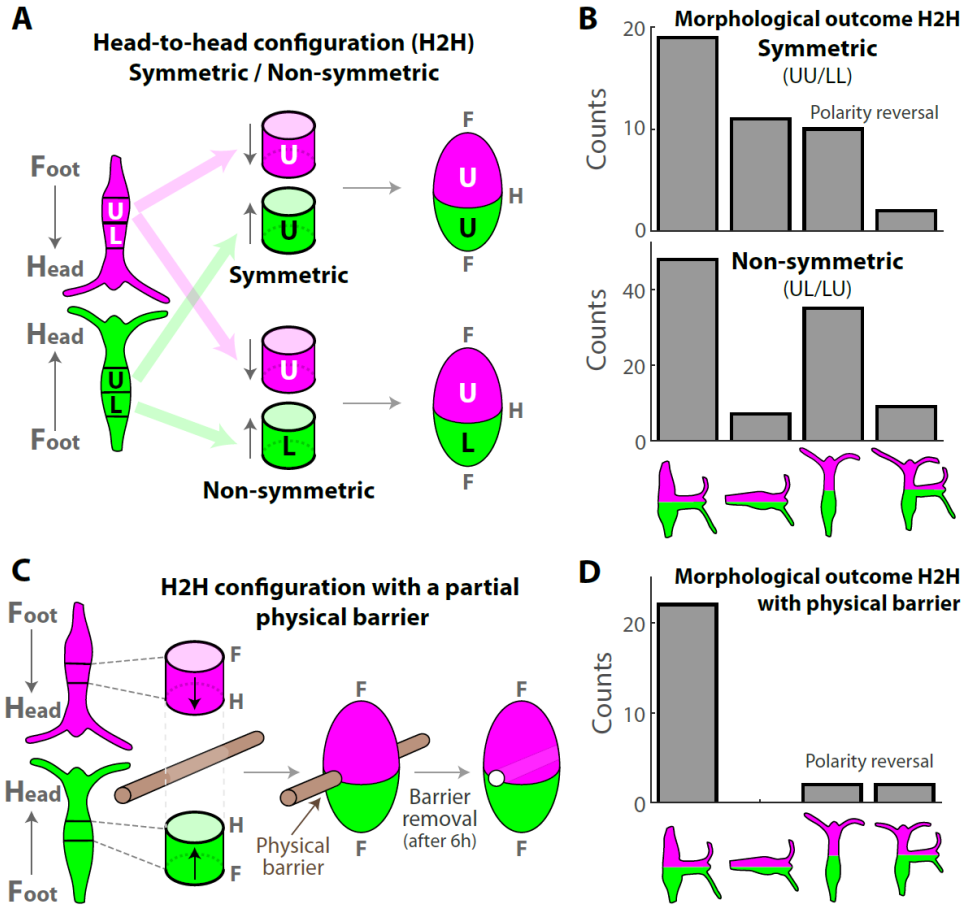

Figure S3. Detailed analysis of the regeneration of H2H doublets. (A) Schematic illustration of the regeneration experiments with fused ring doublets in the H2H configuration. Rings are excised from above (U) or below (L) the approximated midpoint of the two parent animals that are differentially labeled (green/magenta). The rings are fused so that their originally head-facing sides adhere to each other. Samples are made from two rings taken from the same position along the body axis of the parent animals (top; symmetric UU or LL) or from different positions (bottom; non-symmetric UL or LU). (B) Bar plot depicting the outcome morphologies of fused H2H ring doublets generated in a symmetric (UU or LL; top) or non-symmetric (UL or LU; bottom) manner. (C) Schematic illustration of the formation of a H2H doublet with a physical barrier (a 75 µm-diameter wire) placed at the adhesion site. The barrier is removed after ~6 hours and the regeneration proceeds as in (A). (D) Bar plot depicting the outcome morphologies of H2H doublets formed with this physical barrier. The probability for polarity reversal with head formation at an originally foot-facing side of one of the excised rings (right bars) is reduced by the presence of the barrier (compare to (B)).

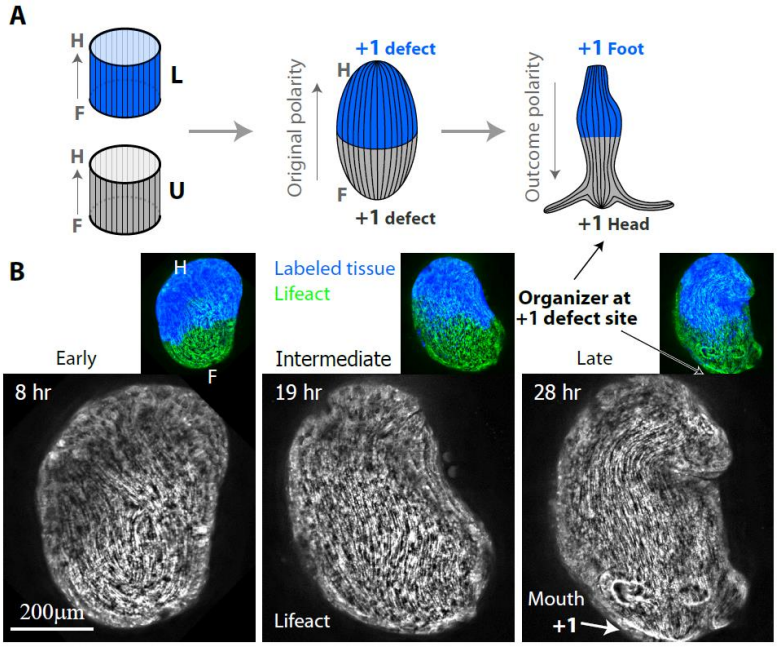

Figure S4. Actin fiber organization in a regenerating H2F ring doublet that undergoes polarity reversal. (A) Schematic illustration of the ectodermal actin fiber organization during regeneration of an anti-oriented H2F ring doublet that undergoes polarity reversal. Left: The actin fibers in the excised rings are arranged in parallel arrays, along the direction of the body axis of their parent animal. The two rings are positioned in an anti-oriented H2F configuration, and one of the rings is marked with a fluorescent tissue label (blue). Middle: Following fusion, the actin fibers from the two rings can join to form continuous fibers that span the length of the fused ring doublet. Two aster-like defects with a net topological charge of +1 (32) form at the top and bottom ends of the ring doublet. Right: In the case of polarity reversal, the fused ring doublet regenerates into an animal that has a normal morphology, with a new head forming at the +1 defect site at the bottom (originally foot-facing) edge of the doublet, and a foot forming at the other (originally head-facing) end. (B) Spinning-disk confocal images from a time-lapse movie of an anti-oriented H2F doublet that underwent polarity reversal. Images are shown at an early (left), intermediate (middle) and late (right) time points during the regeneration process. The projected lifeact-GFP signal (see Methods) shows the organization of the ectodermal actin fibers. The +1 defect site at the bottom edge of the sealed doublet coincides with the formation site of the new organizer at the mouth of the regenerated animal. Insets: Overlay depicting the lifeact-GFP signal (green) together with the fluorescent tissue label that marks one of the fused rings (blue; Texas Red-conjugated 3kD Dextran).